ORIGINAL RESEARCH

# A Noninvasive Imaging Approach to Assess Plaque Severity: The Carotid Atherosclerosis Score

H.R. Underhill
T.S. Hatsukami
J. Cai
W. Yu
J.K. DeMarco
N.L. Polissar
H. Ota
X. Zhao
L. Dong
M. Oikawa
C. Yuan

**BACKGROUND AND PURPOSE:** The presence of IPH and/or FCR in the carotid atherosclerotic plaque indicates a high-risk lesion. The aim of this multicenter cross-sectional study was to establish the characteristics of lesions that may precede IPH and/or FCR. We further sought to construct a CAS that stratifies carotid disease severity.

**MATERIALS AND METHODS:** Three hundred forty-four individuals from 4 imaging centers with 16%–99% carotid stenosis by duplex sonography underwent carotid MR imaging. In approximately 60% of the study sample (training group), multivariate analysis was used to determine factors associated with IPH and FCR. Statistically significant parameters identified during multivariate analysis were used to construct CAS. CAS was then applied to the remaining arteries (40%, test group), and the accuracy of classification for determining the presence versus absence of IPH or, separately, FCR was determined by ROC analysis and calculation of the AUC.

**RESULTS:** The maximum proportion of the arterial wall occupied by the LRNC was the strongest predictor of IPH ($P < .001$) and FCR ($P < .001$) during multivariate analysis of the training group. The subsequently derived CAS applied to the test group was an accurate classifier of IPH (AUC = 0.91) and FCR (AUC = 0.93). Compared with MRA stenosis, CAS was a stronger classifier of both IPH and FCR.

**CONCLUSIONS:** LRNC quantification may be an effective complementary strategy to stenosis for classifying carotid atherosclerotic disease severity. CAS forms the foundation for a simple imaging-based risk-stratification system in the carotid artery to classify severity of atherosclerotic disease.

**ABBREVIATIONS:** AH = Anzhen Hospital; AUC = area-under-the-curve; CAS = Carotid Atherosclerosis Score; CE = contrast-enhanced; CE-MRA = contrast-enhanced MR angiography; CE-T1WI = contrast-enhanced T1-weighted imaging; CI = confidence interval; FCR = fibrous cap rupture; FSE = fast spin-echo; FSPGR = fast SPGR; FSRS = Framingham Stroke Risk Score; IMT = intima-media thickness; Inf = infinite; IPH = intraplaque hemorrhage; JV = jugular vein; LRNC = lipid-rich necrotic core; Max = maximum; MDIR = multisection double inversion recovery; Min = minimum; MRA = MR angiography; MRI = MR imaging; MSU = Michigan State University; NWI = normalized wall index; OR = odds ratio; PD = proton density; PLA = People's Liberation Army General Hospital; QIR = quadruple inversion recovery; ROC = receiver operating characteristics; SPGR = spoiled gradient-recalled echo; T1WI = T1-weighted imaging; T2WI = T2-weighted imaging; TOF = time-of-flight; TVA = total vessel area; UW = University of Washington

Carotid atherosclerotic disease is a leading cause of stroke. Disease severity and risk of stroke have been traditionally determined by measures of luminal occlusion.[1] Findings from randomized prospective investigations, however, have indicated that stenosis may be an uncertain measure of stroke risk in symptomatic patients with <70% stenosis[2] and across all levels of stenoses in asymptomatic patients.[3] Concurrently, atherosclerotic plaques in the coronary arteries associated with sudden cardiac death have been differentiated from lesions not associated with infarcts by histologic findings from within the vessel wall.[4] In accord, considerable effort has been directed at identifying features of the carotid arterial wall that may provide complementary information to lumenography to evaluate disease severity better.

MR imaging of the carotid arteries has been validated with histology to be an effective method to identify and measure atherosclerotic vessel morphology and plaque composition.[5-7] Recent carotid MR imaging–based cross-sectional[8-10] and prospective[11-13] studies of carotid atherosclerosis have offered exciting evidence that among many plaque features, IPH and FCR are some of the key determinants of the high-risk lesion—plaques associated with cerebrovascular events. Beyond the differentiation of high-risk lesions, however, a critical component of disease assessment is the recognition of lesions that may precede the development of IPH and/or FCR. The aim of this multicenter cross-sectional study was to determine which imaging features or combination of imaging features

Received June 19, 2009; accepted after revision November 23.

From the Departments of Radiology (H.R.U., X.Z., L.D., M.O., C.Y.) and Surgery (T.S.H.), University of Washington, Seattle, Washington; Department of Radiology (J.C.), People's Liberation Army General Hospital, Beijing, China; Department of Radiology (W.Y.), Anzhen Hospital, Capital Medical University, Beijing, China; Department of Radiology (J.K.D., H.O.), Michigan State University, East Lansing, Michigan; and Mountain-Whisper-Light Statistical Consulting (N.L.P.), Seattle, Washington.

This work was supported by grants from the National Institutes of Health (R01-HL56874, R01-HL073401, P01-HL072262, R01-HL61851), the American Heart Association's Midwest Affiliate Grant-in-Aid (0855604G), and Michigan State University (OVPRGS 05-IRGP-472).

Please address correspondence to Hunter R. Underhill, MD, Vascular Imaging Lab, University of Washington, 815 Mercer St, Box 358050, Seattle, WA 98109; e-mail: hunterru@u.washington.edu



DOI 10.3174/ajnr.A2007

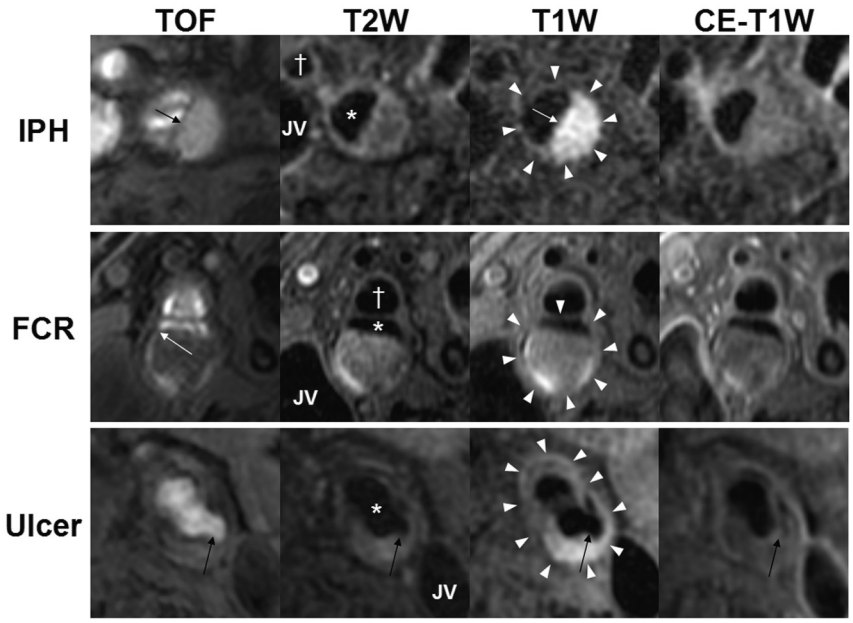


**Fig 1.** In vivo identification of IPH, FCR, and ulceration. Each row contains multicontrast axial images from a single location in the carotid artery. The outer wall boundary (*white arrowheads*) of either the internal or common carotid artery, the lumen of the internal or common (*asterisk*) carotid artery, the external (*cross*, where applicable) carotid artery, and the JV are identified. The top row is of the right internal carotid artery from a 69-year-old man imaged at MSU. IPH (*arrows*) is characterized by a hyperintense signal intensity on TOF and T1WI. The second row is of the right internal carotid artery from an 80-year-old man imaged at PLA. An FCR (*white arrow*) is evident on TOF imaging by the hyperintense signal intensity extending from the lumen into the plaque and the absence of a fibrous cap on T2WI and CE-T1WI. The third row is of the left common carotid artery from a 74-year-old man imaged at PLA. An ulceration (*black arrows*) is present. Notably, the varying appearance of the ulcer between the different contrast weightings is due to reduced flow suppression caused by turbulent flow in the ulcerated region, particularly after contrast administration.

has the highest association with the presence of IPH and/or FCR. We further sought to construct an imaging-based CAS that characterizes features of precursor lesions and provides evidence for an improved method to stratify carotid disease severity compared with the traditional stenosis measurement. This simple scoring system is intended to combine lesion morphologic and compositional information quantitatively, to provide easy tracking of the status of plaques, and to be used in large-scale prospective studies that link plaque features with clinical outcomes.

## Materials and Methods

### *Study Sample*

Multicontrast carotid MR images from 435 individuals with 16%–99% stenosis by duplex sonography in at least 1 carotid artery were pooled from 4 institutions: 1) AH, Capital Medical University, Beijing, China ($n = 78$; stenosis, >50%); 2) MSU, East Lansing, Michigan ($n = 90$; stenosis, >50%); 3) PLA, Beijing, China ($n = 67$; stenosis, >50%); and 4) UW, Seattle, Washington ($n = 80$; stenosis,16%–49%; $n = 120$; stenosis, 50%–79%). The study procedures and consent forms were reviewed and approved by the institutional review board at each institution before study initiation. The artery with the greatest stenosis by duplex sonography, termed the index artery, was selected for image review because image acquisition was centered on that artery. Arteries were excluded from review if there was the following: 1) prior carotid endarterectomy on the index carotid artery, 2) prior radiation therapy to the neck, 3) insufficient coverage (<10 mm including the bifurcation) by MR imaging, or 4) poor image quality by MR imaging. Clinical information was obtained through chart review.

**Table 1: Signal intensity of plaque features across different contrast weightings[a]**

| | TOF | T2WI | PD | T1WI | CE-T1WI |
|---|---|---|---|---|---|
| Calcification | –[b] | –[b] | –[b] | –[b] | – |
| LRNC | o/+ | –/o | –/o | o/+[b] | –[b] |
| IPH | +[b] | –/o | –/o | +[b] | –/o |

[a] Intensity relative to the sternocleidomastoid muscle: – indicates hypointense; o, isointense; +, hyperintense.
[b] Principal criteria for identification of a feature.

### *MR Imaging Acquisition*

Participants underwent carotid MR imaging on either a 1.5T or 3T scanner by using bilateral phased-array carotid surface coils. Previously published multicontrast carotid imaging protocols[14,15] were adapted for each study center. Sequences and imaging parameters are detailed in On-line Table 1. Notably, at 2 sites (AH and MSU) participants also underwent CE-MRA (On-line Table 1).

### *Image Analysis*

All images of the index carotid artery from each subject were interpreted at a core laboratory by teams of 2 reviewers, all with >1.5 years' experience in vascular MR imaging, via consensus opinion and blinded to clinical information. At each axial location, image quality was assessed with a 4-point scale (1 = poor, 2 = adequate, 3 = good, 4 = excellent). For arteries with image quality ≥2, image analysis software[16] was used to draw the lumen and outer wall boundaries at each axial location. Lumen area, wall area, total vessel area, maximum wall thickness, and NWI (wall area/total vessel area) were recorded. In addition, the presence or absence of calcification, LRNC, IPH (Fig 1, top row), and fibrous cap status was determined by using multicontrast imaging criteria that have been previously validated with histol-

ogy[6,17-19] and collectively depicted in a recently published atlas of carotid MR imaging and histology.[20]

Signal-intensity criteria for identifying calcification, LRNC, and IPH are summarized in Table 1. Fibrous cap status was identified as 1) intact thick if fibrous tissue was evident on CE-T1WI or T2WI between the LRNC and the lumen, 2) intact thin if fibrous tissue was not evident on CE-T1WI or T2WI between the LRNC and lumen, and 3) ruptured if there was an absence of a fibrous cap on CE-T1WI and T2WI and juxtaluminal IPH on TOF (Fig 1, middle row). Area measurements of the LRNC and calcification, when present, were also collected, and the proportion of each component relative to the wall area (eg, percentage LRNC area = 100% × LRNC area / wall area) was subsequently calculated for each MR imaging location. Proportional measurements of plaque composition normalized the data for arterial size. Percentage stenosis was determined from the CE-MRA by using the established North American Symptomatic Carotid Endarterectomy Trial criterion[21]: 100% × (1 − luminal diameter at the point of maximal narrowing / the diameter of the normal distal internal carotid artery).

### *Statistical Analysis*

All statistical analyses were performed with SPSS for Windows (Version 12.0, SPSS, Chicago, Illinois). Due to differences among institutions in longitudinal coverage of the artery, the maximum arterial value for each continuous metric was used during data analysis (as opposed to mean arterial values or volume data), except for lumen area, in which case the minimum arterial value was used. Individuals with ulceration, defined as a surface disruption with invagination into the plaque, were excluded from analysis (Fig 1, bottom row). Ulceration alters the morphology and composition of the plaque, which obscures the conditions that existed before the development of ulceration. To account for differences among imaging protocols, field-strengths, and patient demographics at different sites, we randomly divided the remaining evaluable study sample into 2 datasets with an intended ratio of 60:40 (training set/test set) by using the random selection of data command in SPSS. This method of creating a training and test set through random subselection creates 2 datasets that are equivalent to 2 independent random draws from the source collection of patients.[22] Although measures of reproducibility for carotid MR imaging parameters have been previously reported (intra- and inter-reader[6,19]; interscan[15,23,24]), partitioning of the dataset in this manner, after image interpretation had been complete for all arteries, enabled the unbiased evaluation of reproducibility of the results obtained from the training set on the test set. To verify the randomness of allocation between the training and test sets, we evaluated differences in the baseline demographic and arterial characteristics with the independent *t* test for continuous variables and the Fisher exact test for categoric variables. Statistical significance, based on 2-sided tests, was defined as $P < .05$.

The CAS was constructed via the following steps: Step 1, with the training set, univariate binary logistic regression for continuous variables or the Fisher exact test for categoric variables was used to identify potential predictors of IPH and FCR from each of the clinical and arterial parameters listed in Table 2. IPH and FCR were not considered in the univariate analysis because they were the target, dependent variables used as indicators of a high-risk lesion. Step 2, with the training set, we created a multivariate model separately for IPH and FCR by using backward elimination of predictor variables, starting from all parameters with an association ($P < .10$) identified during univariate analysis and by using $P < .10$ (*F* test) to retain a variable in the model. OR and the 95% CI are reported for results from univariate and multivariate analysis. Step 3, by using the training set, we assessed the accuracy of classification for each statistically significant parameter selected in the multivariate analysis with ROC curves and the AUC. Step 4, parameters identified during multivariate analysis of the training set were used to construct the CAS. Notably, methods used to construct the CAS were dependent on the results and are, thus, described in the "Results" section. Step 5, after formulation of the CAS from the training set was complete, performance of CAS was evaluated with the test set. ROC curves and AUC were used to determine the strength of the classification for identifying lesions with IPH or, separately, FCR in the test set.

Prevalence of calcification, LRNC, IPH, and fibrous cap status (thick, thin, or ruptured) are reported for each level of CAS separately for the training and the test sets. The prevalence of IPH, FCR, and measures used to construct the CAS were computed at each imaging location (relative to the bifurcation) for the entire dataset (training + test). Finally, in all participants with a CE-MRA, strength of classification for determining the presence of IPH and FCR was determined for both MRA stenosis and CAS.

**Table 2: Demographic information ($n = 334$)**

| | Training Set ($n = 196$) | Testing Set ($n = 138$) | *P* Value |
|---|---|---|---|
| Age (yr) | 69.0 ± 10.1 | 69.5 ± 9.5 | .61 |
| Male sex (%) | 74.0 | 76.1 | .70 |
| History of | | | |
| Hypertension (%) | 79.1 | 75.2 | .43 |
| Diabetes mellitus (%) | 20.4 | 27.5 | .15 |
| Coronary artery disease (%) | 34.3 | 39.3 | .41 |
| Smoking status | | | |
| Never (%) | 28.2 | 31.9 | .59 |
| Quit (%) | 49.7 | 44.2 | |
| Current (%) | 22.1 | 23.9 | |
| Imaging center | | | |
| AH (%) | 19.9 | 21.7 | .27 |
| MSU (%) | 21.4 | 13.0 | |
| PLA (%) | 13.8 | 15.9 | |
| UW (%) | 44.9 | 49.3 | |
| Intraplaque hemorrhage (%) | 24.0 | 19.6 | .35 |
| Fibrous cap rupture (%) | 7.1 | 10.9 | .24 |
| Min lumen area ($mm^2$) | 17.2 ± 10.4 | 17.9 ± 9.1 | .51 |
| Max wall area ($mm^2$) | 61.1 ± 21.6 | 63.8 ± 24.5 | .29 |
| Max total vessel area ($mm^2$) | 113.0 ± 35.7 | 117.4 ± 38.3 | .29 |
| Max wall thickness ($mm^2$) | 3.93 ± 1.79 | 4.00 ± 1.70 | .72 |
| Max normalized wall index | 0.696 ± 0.139 | 0.674 ± 0.142 | .16 |
| Presence of calcification (%) | 72.4 | 73.9 | .80 |
| Max percentage calcification (%)[a] | 14.7 ± 10.4 | 16.1 ± 10.7 | .31 |
| Presence of LRNC (%) | 59.7 | 63.7 | .49 |
| Max percentage LRNC[a] (%) | 35.8 ± 18.3 | 31.3 ± 17.9 | .09 |
| MRA stenosis (%) | 47.6 ± 29.3 | 48.8 ± 32.4 | .83 |

[a] Only for arteries with calcification ($n = 244$) or LRNC ($n = 206$) present.

## Results

Of the 435 index arteries available for review, 388 (89.2%) had ≥10-mm longitudinal coverage, which included the bifurcation and sufficient image quality for identification of the vessel boundaries and plaque composition. An additional 54 arteries were excluded due to the presence of ulceration on the index artery. The remaining 334 arteries were used to form the training and testing datasets. Of these 334 arteries, 116 arteries had corresponding CE-MRA from AH and MSU. The mean lon-

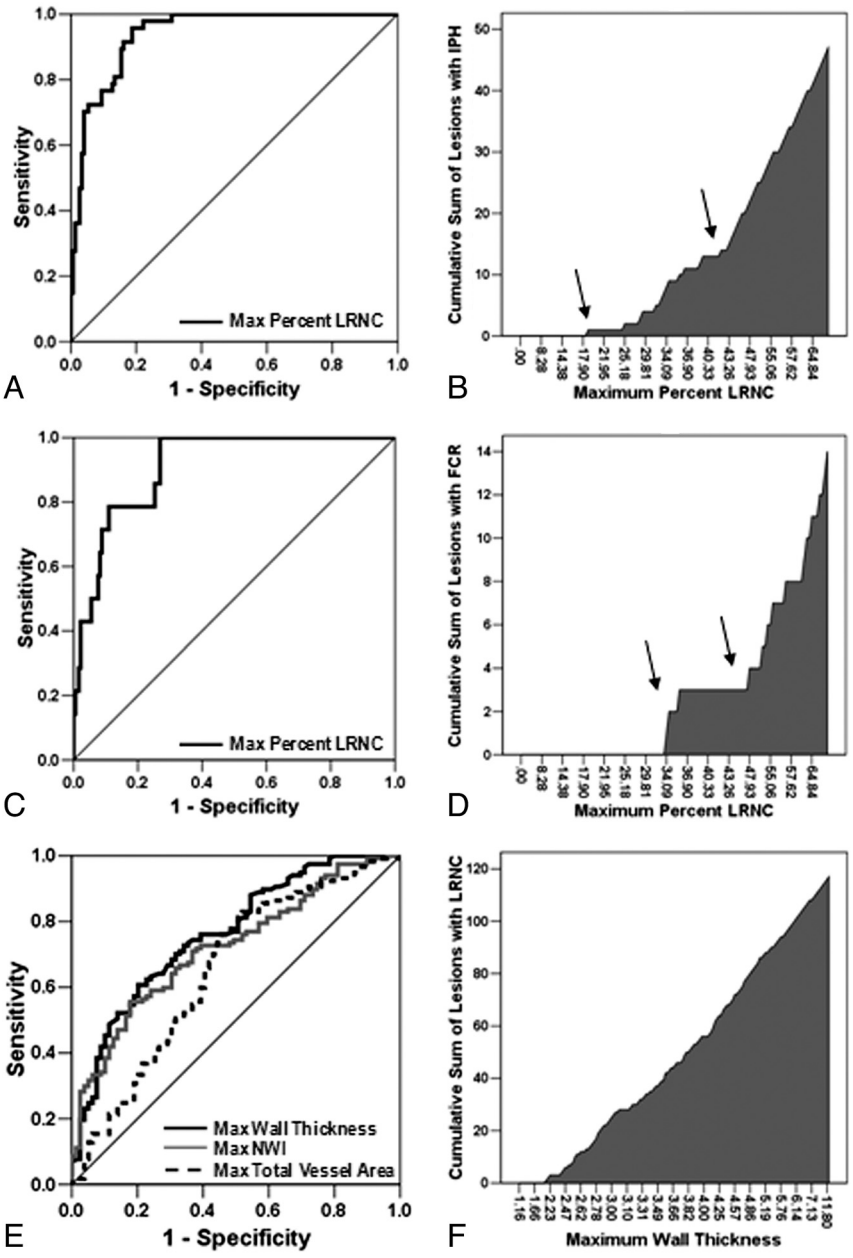


**Fig 2.** ROC curve analyses for the classification of IPH (*A*) and FCR (*C*) in the training set by maximum percentage LRNC. Adjacent to each ROC curve is a cumulative prevalence plot for IPH (*B*) and FCR (*D*) versus maximum percentage LRNC. The cumulative prevalence plots clearly depict changes in slope (*arrows*) for both IPH (*B*) and FCR (*D*), which were subsequently used to construct the CAS. *E*, ROC curve analysis for prediction of the presence of LRNC in the training set by maximum wall thickness, maximum total vessel area, and maximum NWI. *F*, In the cumulative prevalence plot for LRNC by maximum wall thickness, LRNC was absent in lesions with a maximum wall thickness <2 mm.

gitudinal coverage of the 334 evaluable scans was 23.4 ± 7.8 mm (range, 10–36 mm). There were no significant differences in demographic data, arterial morphology, and plaque composition between the training and test groups (Table 2).

Metrics that were associated with the presence of IPH or FCR, as identified during univariate analyses of the training set, are presented in On-line Table 2. Analysis in the training set through backward elimination in multivariate logistic regression selected the maximum percentage LRNC as the sole statistically significant predictor of both IPH (OR for 10% increase in maximum percentage LRNC, 3.3; 95% CI, 2.3–4.7; $P < .001$) and FCR (OR for 10% increase in maximum percentage LRNC, 2.5; 95% CI, 1.6–3.8; $P < .001$). Of note, MRA stenosis was available for only a subset of arteries in the training set, so multivariate analysis was performed twice for FCR: 1) on the subset of arteries for which MRA stenosis could be used as a covariate. and 2) on the entire training set without MRA stenosis as a covariate. In both instances, maximum percentage LRNC was the sole statistically significant predictor of FCR. ROC analysis of the training set found maximum percentage LRNC to be a strong classifier of both IPH (AUC = 0.94, Fig 2*A*) and FCR (AUC = 0.91, Fig 2*C*).

### *CAS*

In evaluating the cumulative prevalence of IPH at different levels of maximum percentage LRNC within the training set, the curve (shown in Fig 2*B*) showed 2 distinguishable jumps at approximately 20% and 40%. Evidentiary change in the cu-

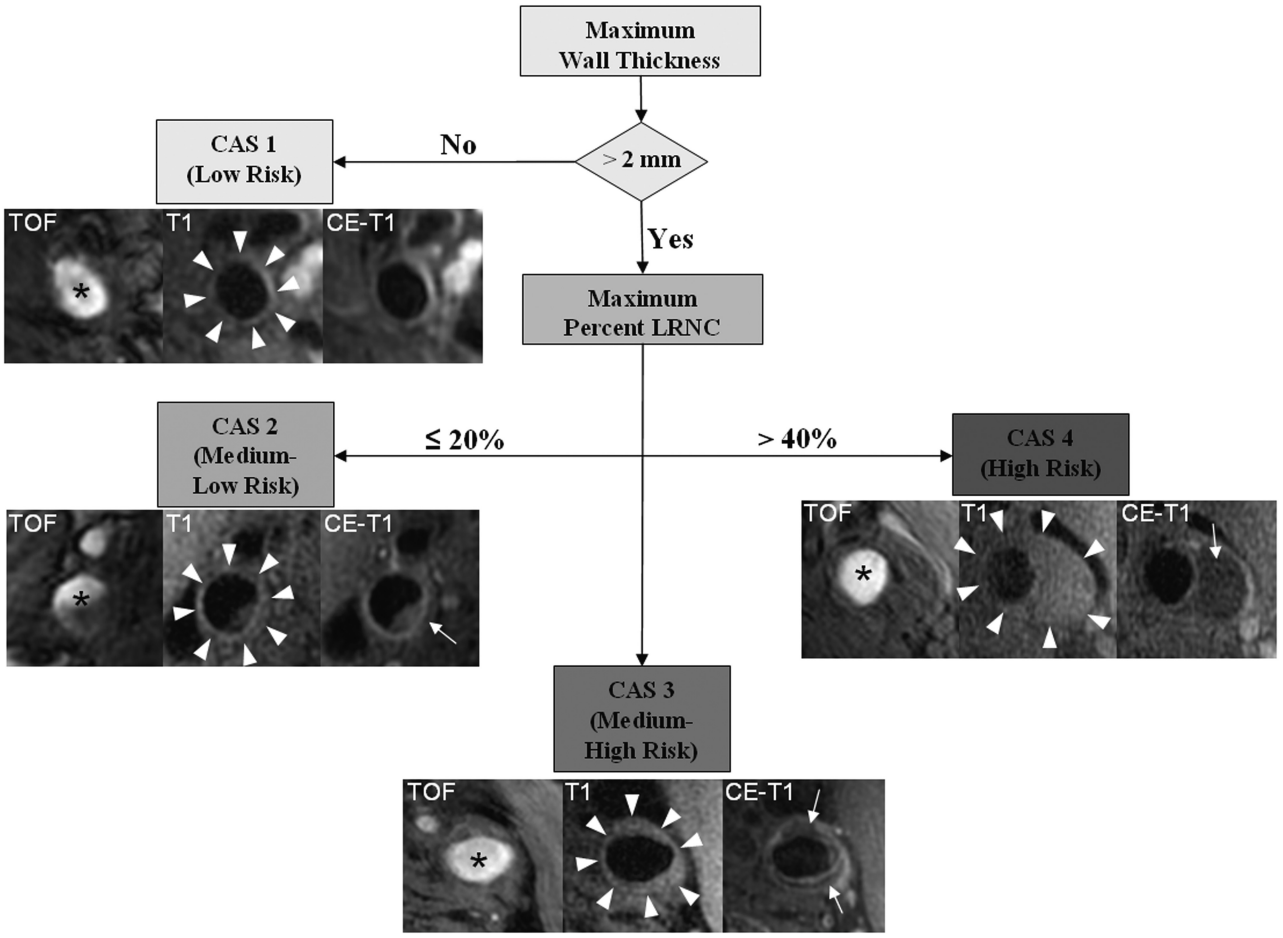


**Fig 3.** Flow diagram of CAS. Subjects with a maximum wall thickness >2 mm require additional evaluation. Further categorization of lesions can be determined by the size of the maximum percentage LRNC. Examples of matched cross-sectional images from 3 contrast weightings (TOF, T1WI, and CE-T1WI) for each category are provided. Images corresponding to CAS 1 (maximum wall thickness <2 mm) are from the left common carotid artery of a 69-year-old man imaged at MSU. The plaque in the CAS 2 (maximum percentage LRNC, ≤20%) example is from the right internal carotid artery of a 63-year-old man imaged at UW. There is a small LRNC (*arrow*) present on postcontrast imaging. Of note, there are also flow artifacts visible in the lumen—common artifacts in images distal to the bifurcation. The lesion in CAS 3 (maximum percentage LRNC, >20% and ≤40%) is from the left common carotid artery of a 65-year-old man imaged at AH. A noticeable LRNC (*arrows*) is present in both the anterior and posterior arterial wall. An example of a large LRNC (*arrow*) without IPH in the left common carotid artery of a 64-year-old man imaged at PLA is shown for CAS 4 (maximum percentage LRNC, >40%). Arrowheads indicate the outer wall boundary; asterisk, the lumen.

**Table 3: Prevalence of features for each level of CAS**

| | 1 | 2 | 3 | 4 |
|---|---|---|---|---|
| Training set ($n$ = 196) | | | | |
| No. | 16 | 90 | 42 | 48 |
| Calcification (%) | 12.5 | 80.0 | 78.6 | 72.9 |
| LRNC (%) | 0.0 | 30.0 | 100.0 | 100.0 |
| IPH (%) | 0.0 | 1.1 | 28.6 | 70.8 |
| Fibrous cap status | | | | |
| Thick (%) | 0.0 | 21.1 (66.7)[a] | 23.8 | 12.5 |
| Thin (%) | 0.0 | 10.0 (33.3)[a] | 69.1 | 64.6 |
| Ruptured (%) | 0.0 | 0.0 | 7.1 | 22.9 |
| Testing Set ($n$ = 138) | | | | |
| No. | 17 | 62 | 34 | 25 |
| Calcification (%) | 17.6 | 83.9 | 79.4 | 80.0 |
| LRNC (%) | 11.8 | 43.5 | 100.0 | 100.0 |
| IPH (%) | 0.0 | 0.0 | 29.4 | 68.0 |
| Fibrous cap status | | | | |
| Thick (%) | 11.8 (100.0)[a] | 30.7 (66.7)[a] | 29.4 | 4.0 |
| Thin (%) | 0.0 | 14.5 (33.3)[a] | 64.7 | 44.0 |
| Ruptured (%) | 0.0 | 0.0 | 5.9 | 52.0 |

[a] Lesions with an LRNC.

mulative prevalence of FCR occurred at maximum percentage LRNC values equal to approximately 30% and 45% (Fig 2*D*). Thus, cutoff values for maximum percentage LRNC were selected at 20% and 40% to provide 3 tiers (<20%, 20%–40%, and >40%) of stratification of risk for both IPH and FCR.

Because only lesions with an LRNC would be eligible for classification beyond the first tier, an additional univariate/multivariate analysis was performed to determine predictors of the presence of an LRNC (On-line Table 2). Among the 3 variables identified during multivariate analysis (On-line Table 2), accuracy of classification of arteries (LRNC present versus absent, Fig 2*E*) was strongest for maximum wall thickness (AUC = 0.76), followed by maximum NWI (AUC = 0.72) and maximum total vessel area (AUC = 0.65). From a plot of cumulative prevalence of arteries with LRNC versus maximum wall thickness for the training set (Fig 2*F*), LRNC did not occur in arteries with a maximum wall thickness ≤2 mm. As such, lesions with a maximum wall thickness ≤2 mm were classified as the first tier of CAS followed by the 3 tiers dependent on the size of the maximum percentage LRNC (Fig 3).

Applied to the test set ($n$ = 138), the 4-tier CAS was a strong classifier of both IPH (AUC = 0.91) and FCR (AUC = 0.93). The prevalence of each compositional feature for each

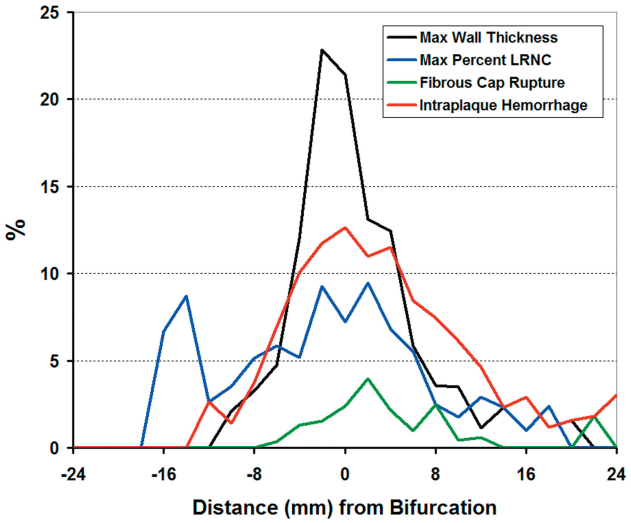


**Fig 4.** Prevalence of key features in the carotid artery is shown for each MR imaging location relative to the bifurcation. Distance from the bifurcation (0) is labeled on the x-axis, where positive and negative integers represent locations within the internal and common carotid arteries, respectively.

category of CAS applied to both the training and test sets is detailed in Table 3.

### *Anatomic Location of Key Features*

An analysis of the prevalence of plaque features at different locations in the artery, including all evaluable arteries without an ulcer ($n = 3898$ sections from 334 arteries) demonstrated that the maximum wall thickness and maximum percentage LRNC, IPH, and FCR occurred predominately at or adjacent to the carotid bifurcation (Fig 4).

### *CAS versus MRA Percentage Stenosis*

In the subcohort of individuals with CE-MRA ($n = 116$), CAS was a stronger classifier than stenosis for both IPH (AUC = 0.87 versus 0.57, respectively; Fig 5*A*) and FCR (AUC = 0.85 versus 0.67, respectively; Fig 5*B*).

## Discussion

This study used a standardized carotid MR imaging protocol implemented at multiple centers to evaluate a spectrum of in vivo carotid atherosclerotic disease. While carotid MR imaging enables the assessment of a multitude of morphologic and compositional imaging parameters, this cross-sectional study distinguished the maximum percentage LRNC as the variable with the strongest association with the presence of IPH and FCR. In addition, our data indicate that in the absence of high-risk features (IPH, FCR, and/or ulceration), plaques with a maximum percentage LRNC >40% may also be considered high-risk (CAS 4) due to the high prevalence of IPH and/or FCR observed in this subset of arteries. A simple imaging-based risk assessment system derived from these findings, such as CAS, may prove clinically useful for stratifying atherosclerotic disease severity in the carotid artery. These results form the basis for large prospective studies that target the LRNC as the key parameter for determining the risk of developing IPH and/or FCR and for evaluating the risk of cerebrovascular events along with IPH, FCR, ulceration, and stenosis.

Compared with stenosis, the traditional measure of carotid atherosclerotic disease severity, CAS was a stronger classifier for the presence of IPH and FCR. Outward remodeling[25] coupled with an enlarged luminal area of the carotid bulb, the location where these features were most prevalent (Fig 4), may enable the development of high-risk features before detectable luminal encroachment. Babiarz et al[26] described a wide range of plaque burden in lesions with minimal stenosis as determined by CE-MRA. Saam et al[27] found that IPH or FCR or both were present in 8.7% of lesions with 1%–15% stenosis and 21.7% of lesions with 16%–49% stenosis. Most recently, Dong et al[28] reported the occurrence of both IPH and FCR in angiographically normal (0% stenosis) arteries. Collectively, these previous studies[26-28] highlight the potential limitations of traditional risk-stratification systems that use stenosis as the principal criterion for discriminating lesion severity. Accordingly, alternate methods for assessing carotid atherosclerotic disease severity, such as CAS, may be clinically constructive, particularly in patients with <70% stenosis.

Our findings demonstrated that arterial wall thickness measurements were effective for discriminating between lesions with and without a LRNC. This is interesting because it may create a natural connection point between sonography and MR imaging in a clinical setting. Measures of carotid wall thickness by sonography have been previously associated with stroke. O'Leary et al[29] found that a maximum internal carotid IMT ≥1.81 mm was associated with an adjusted relative risk of 2.4 for incident stroke. Touboul et al[30] found the presence of

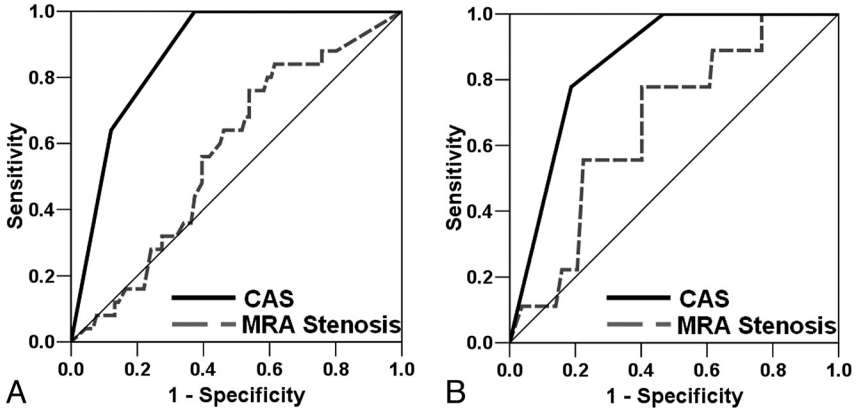


**Fig 5.** ROC curve analyses for IPH (*A*) and FCR (*B*) by using either CAS or MRA stenosis.

carotid plaque that encroached into the vessel >1 mm to be independently associated with stroke risk. However, discrimination of plaque stability solely on morphology (eg, wall thickness) may be insufficient. Prati et al[31] recently reported that inclusion of carotid findings (eg, IMT >1 mm and at least 1 plaque) into the FSRS resulted in a higher predictive power of incident stroke only in subjects with an FSRS >20%. Accordingly, we found wall thickness to be an appropriate measure for differentiation between stable and potentially unstable carotid disease, but parameters beyond arterial morphology were necessary to classify severity accurately. Nevertheless, evaluation of wall thickness measurements, particularly with sonography, may be a cost-effective strategy for identifying individuals to evaluate with multicontrast high-resolution carotid MR imaging.

There are several limitations that merit discussion. First, the imaging protocol used in this study was not uniform across study centers. However, randomly partitioning the data into training and test sets accounts for differences that may occur due to the site. Furthermore, the heterogeneity within the dataset suggests that CAS may be sufficiently robust to overcome differences that may occur as a result of image acquisition. Second, the current CAS is limited to predicting the presence of IPH and FCR in the carotid atherosclerotic lesion. While the scoring system may require further optimization based on future prospective studies linked to clinical (eg, stroke) and/or imaging (eg, development of a new IPH) outcomes, the proposed system may already be relevant. The data presented herein and the subsequently derived CAS point to ways to improve carotid MR imaging efficiency and accuracy by focusing imaging strategies on the detection of the LRNC, IPH, FCR, and ulceration. Sequences used during this investigation were part of a broad multicontrast protocol to comprehensively evaluate carotid disease. Selecting sequences to focus on quantification of the specific features (eg, CE-T1WI[18] for LRNC; TOF[19] or magnetization-prepared rapid acquisition of gradient echo[32] for IPH) necessary for severity assessment may substantially decrease scanning time and increase translatability of carotid MR imaging to clinical practice.

Finally, CAS was not applied to neurologic symptom status. Because patient examinations were pooled from multiple different institutions, inclusion criteria for the carotid MR imaging varied. For example, only asymptomatic patients were imaged at UW compared with MSU, which imaged both asymptomatic and symptomatic individuals. In addition, findings from several large population-based studies indicate a much greater prevalence of subclinical strokes compared with clinically overt events.[33,34] To accurately determine the ability of CAS to classify risk, future prospective investigations should integrate brain MR imaging to account for all strokes (silent and overt) that occur within the carotid vascular supply.

## Conclusions

We conclude that the maximum percentage LRNC is an effective parameter for classifying the severity of carotid atherosclerotic disease. In the absence of FCR, IPH, and ulceration, a plaque with a maximum percentage LRNC >40% may be a high-risk lesion. The findings from this cross-sectional study form the basis for large long-term prospective studies that evaluate the effectiveness of CAS in predicting disease progression, development of FCR and IPH, and future ischemic events.

## References


1. Moore WS, Barnett HJ, Beebe HG, et al. **Guidelines for carotid endarterectomy: a multidisciplinary consensus statement from the Ad Hoc Committee, American Heart Association.** *Circulation* 1995;91:566–79
2. Barnett HJ, Taylor DW, Eliasziw M, et al. **Benefit of carotid endarterectomy in patients with symptomatic moderate or severe stenosis: North American Symptomatic Carotid Endarterectomy Trial Collaborators.** *N Engl J Med* 1998;339:1415–25
3. **Endarterectomy for asymptomatic carotid artery stenosis: Executive Committee for the Asymptomatic Carotid Atherosclerosis Study**. *JAMA* 1995;273:1421–28
4. Virmani R, Kolodgie FD, Burke AP, et al. **Lessons from sudden coronary death: a comprehensive morphological classification scheme for atherosclerotic lesions.** *Arterioscler Thromb Vasc Biol* 2000;20:1262–75
5. Toussaint JF, LaMuraglia GM, Southern JF, et al. **Magnetic resonance images: lipid, fibrous, calcified, hemorrhagic, and thrombotic components of human atherosclerosis in vivo.** *Circulation* 1996;94:932–38
6. Saam T, Ferguson MS, Yarnykh VL, et al. **Quantitative evaluation of carotid plaque composition by in vivo MRI.** *Arterioscler Thromb Vasc Biol* 2005;25:234–39
7. Fayad ZA, Fuster V. **Characterization of atherosclerotic plaques by magnetic resonance imaging.** *Ann N Y Acad Sci* 2000;902:173–86
8. Murphy RE, Moody AR, Morgan PS, et al. **Prevalence of complicated carotid atheroma as detected by magnetic resonance direct thrombus imaging in patients with suspected carotid artery stenosis and previous acute cerebral ischemia.** *Circulation* 2003;107:3053–58
9. Yuan C, Zhang SX, Polissar NL, et al. **Identification of fibrous cap rupture with magnetic resonance imaging is highly associated with recent transient ischemic attack or stroke.** *Circulation* 2002;105:181–85
10. Saam T, Cai J, Ma L, et al. **Comparison of symptomatic and asymptomatic atherosclerotic carotid plaque features with in vivo MR imaging.** *Radiology* 2006;240:464–72
11. Altaf N, Daniels L, Morgan PS, et al. **Detection of intraplaque hemorrhage by magnetic resonance imaging in symptomatic patients with mild to moderate carotid stenosis predicts recurrent neurological events.** *J Vasc Surg* 2008;47:337–42
12. Takaya N, Yuan C, Chu B, et al. **Association between carotid plaque characteristics and subsequent ischemic cerebrovascular events: a prospective assessment with MRI—initial results.** *Stroke* 2006;37:818–23
13. Singh N, Moody AR, Gladstone DJ, et al. **Moderate carotid artery stenosis: MR imaging-depicted intraplaque hemorrhage predicts risk of cerebrovascular ischemic events in asymptomatic men.** *Radiology* 2009;252:502–08
14. Yuan C, Kerwin WS, Yarnykh VL, et al. **MRI of atherosclerosis in clinical trials.** *NMR Biomed* 2006;19:636–54
15. Underhill HR, Yarnykh VL, Hatsukami TS, et al. **Carotid plaque morphology and composition: initial comparison between 1.5- and 3.0-T magnetic field strengths.** *Radiology* 2008;248:550–60
16. Kerwin W, Xu D, Liu F, et al. **Magnetic resonance imaging of carotid atherosclerosis: plaque analysis.** *Top Magn Reson Imaging* 2007;18:371–78
17. Hatsukami TS, Ross R, Polissar NL, et al. **Visualization of fibrous cap thickness and rupture in human atherosclerotic carotid plaque in vivo with high-resolution magnetic resonance imaging.** *Circulation* 2000;102:959–64
18. Cai J, Hatsukami TS, Ferguson MS, et al. **In vivo quantitative measurement of intact fibrous cap and lipid-rich necrotic core size in atherosclerotic carotid plaque: comparison of high-resolution, contrast-enhanced magnetic resonance imaging and histology.** *Circulation* 2005;112:3437–44
19. Chu B, Kampschulte A, Ferguson MS, et al. **Hemorrhage in the atherosclerotic carotid plaque: a high-resolution MRI study.** *Stroke* 2004;35:1079–84
20. Chu B, Ferguson MS, Chen H, et al. **Cardiac magnetic resonance features of the disruption-prone and the disrupted carotid plaque.** *JACC Cardiovasc Imaging* 2009;2:883–96
21. **Beneficial effect of carotid endarterectomy in symptomatic patients with high-grade carotid stenosis: North American Symptomatic Carotid Endarterectomy Trial Collaborators**. *N Engl J Med* 1991;325:445–53
22. Harrell FE Jr, Lee KL, Califf RM, et al. **Regression modelling strategies for improved prognostic prediction.** *Stat Med* 1984;3:143–52
23. Saam T, Kerwin WS, Chu B, et al. **Sample size calculation for clinical trials using magnetic resonance imaging for the quantitative assessment of carotid atherosclerosis.** *J Cardiovasc Magn Reson* 2005;7:799–808
24. Underhill HR, Yuan C, Zhao XQ, et al. **Effect of rosuvastatin therapy on carotid plaque morphology and composition in moderately hypercholesterolemic patients: a high-resolution magnetic resonance imaging trial**. *Am Heart J* 2008;155:584 e581–88. Epub 2008 Jan 18

25. Glagov S, Weisenberg E, Zarins CK, et al. **Compensatory enlargement of human atherosclerotic coronary arteries.** *N Engl J Med* 1987;316:1371–75
26. Babiarz LS, Astor B, Mohamed MA, et al. **Comparison of gadolinium-enhanced cardiovascular magnetic resonance angiography with high-resolution black blood cardiovascular magnetic resonance for assessing carotid artery stenosis.** *J Cardiovasc Magn Reson* 2007;9:63–70
27. Saam T, Underhill HR, Chu B, et al. **Prevalence of American Heart Association type VI carotid atherosclerotic lesions identified by magnetic resonance imaging for different levels of stenosis as measured by duplex ultrasound.** *J Am Coll Cardiol* 2008;51:1014–21
28. Dong L, Underhill HR, Yu W, et al. **Geometric and compositional appearance of atheroma in an angiographically normal carotid artery in patients with atherosclerosis**. *AJNR Am J Neuroradiol* 2010;31:311–16
29. O'Leary DH, Polak JF, Kronmal RA, et al. **Carotid-artery intima and media thickness as a risk factor for myocardial infarction and stroke in older adults: Cardiovascular Health Study Collaborative Research Group.** *N Engl J Med* 1999;340:14–22
30. Touboul PJ, Labreuche J, Vicaut E, et al. **Carotid intima-media thickness, plaques, and Framingham risk score as independent determinants of stroke risk.** *Stroke* 2005;36:1741–45
31. Prati P, Tosetto A, Vanuzzo D, et al. **Carotid intima media thickness and plaques can predict the occurrence of ischemic cerebrovascular events.** *Stroke* 2008;39:2470–76
32. Moody AR, Murphy RE, Morgan PS, et al. **Characterization of complicated carotid plaque with magnetic resonance direct thrombus imaging in patients with cerebral ischemia.** *Circulation* 2003;107:3047–52
33. Bryan RN, Cai J, Burke G, et al. **Prevalence and anatomic characteristics of infarct-like lesions on MR images of middle-aged adults: the atherosclerosis risk in communities study.** *AJNR Am J Neuroradiol* 1999;20:1273–80
34. Manolio TA, Kronmal RA, Burke GL, et al. **Magnetic resonance abnormalities and cardiovascular disease in older adults: The Cardiovascular Health Study.** *Stroke* 1994;25:318–27
35. Yarnykh VL, Yuan C. **T1-insensitive flow suppression using quadruple inversion-recovery.** *Magn Reson Med* 2002;48:899–905
36. Yarnykh VL, Yuan C. **Multislice double inversion-recovery black-blood imaging with simultaneous slice reinversion.** *J Magn Reson Imaging* 2003;17:478–83